Int. J. Electrochem. Sci., 8 **(2013)** 678 - 688

International Journal of
ELECTROCHEMICAL
SCIENCE
www.electrochemsci.org

Preparation of Protective Ni-Al Coating on Low Carbon Steel by Pulsed Composite Electrodeposition

S.D. Chen, J. Zhao[*]

School of Applied Chemistry, Shenyang University of Chemical Technology, 11th street, 110142, Shenyang, China
[*]E-mail: zhaojinspider@qq.com

Received: 27 October 2012 / *Accepted:* 29 November 2012 / *Published:* 1 January 2012

Pulsed composite electrodeposition and interdiffusion treatment were used to develop a Ni-Al protective coating on low carbon steel. The morphology and microstructure of the coating were investigated with SEM and XRD. The coating is composed of a continuous Ni-rich phase and discrete Al-rich particles enclosed in the Ni-rich phase. The corrosion-resistant coating exhibits excellent adhesion to the steel substrate due to the formation of Ni-Al intermetallics. The optimized processing parameters such as duty cycle of 2, pulse frequency of 800 Hz, and current density of 3 A/dm^2 were determined.

Keywords: Composite electro-deposition; Pulse plating; Ni-coated Al powders; Heat treatment

1. INTRODUCTION

Ordinary carbon steels have been widely used as structural materials in many fields because of their economy and convenience of machining, but they can be easily rotted in moist, acid, alkali, and high-temperature environments. Surface coating is a commonly used method for improving the corrosion/oxidation resistance in various aggressive environments of the low carbon steels without altering the bulk properties. For example, hot dip galvanizing has been extensively used for the protection of low carbon steels against atmospheric corrosion [1-3]. The replacement of molten Zn by Zn alloys can improve the corrosion resistance [4-6]. In addition, hot dip aluminizing has been also widely used, and it is able to provide oxidation resistance at high temperatures [7, 8].

Besides the hot dipping, extensive attempts on electrodeposition have been taken to develop highly corrosion resistant coatings on the low carbon steels [9-15]. Most of the reported results involve the fabrication of Zn-based alloy coatings on the steels. To enhance the high temperature corrosion resistance, it is necessary to introduce some beneficial elements, such as Al, into the coatings during

the electrodepositing. Although the electrodeposition of Al metal in water solutions is rather difficult because of the high electropositivity of Al, some authors were successful in fabricating Ni-Al composite coatings on various of substrates through electrodeposition under proper conditions [16-20]. In this paper, a Ni-Al composite coating is prepared on low carbon steel using the pulsed composite electrodeposition and subsequent interdiffusion treatment.

2. EXPERIMENTAL

2.1. Chemical plating of nickel on aluminum powders

The formulation and process parameters of chemical plating nickel are as follows: spherical aluminum powders [grain size: 13 ± 2 μm, the materials fit GB1196 melting level aluminum standard (AL99.7), chemical composition of the aluminum powder: Al > 98.00%, Mn 0.015%, Cu 0.200%, Fe 0.200%, Si 0.100%]. 250 g/L nickel sulfuric, 35 g/L sodium citric acid, 9 g/L citric acid, 90 g/L sodium hypophosphite, 4 g/L thiourea, ammonia water (26 ~ 28%) at right amount, pH: 10.0 ~ 11.2, temperature: 80 ~ 90 ^{o}C, plating time: 4 h.

2.2. Composite electrodeposition of nickel-coated aluminum powders

Cathode is 1.0 cm × 2.0 cm × 0.2 cm of A3 steel plate, with the process of deoil, acid erosion, pulse plating nickel-coated aluminum, washed after finish every step. The anode: 1.0 cm × 2.0 cm, thin and pure nickel piece (Ni > 99.9%), Dipped into the 60 ^{o}C pickling solution about 60 s, removed oil, washed, then acetone-washed and dried. Plating solution composition and process conditions: $NiSO_4$ 300.0 ~ 333.0 g/L, $MgSO_4$ 9.8 ~ 14.7 g/L, NaCl 10.0 ~ 20.0 g/L, H_3BO_3 30.0 ~ 40.0 g/L, $H_2C_2O_4$ 18.0 ~ 26.0 g/L, OP10 0.5 ~ 1.0 g/L, nickel-coated aluminum 25.0 ~ 40.0 g/L, pH 4.7 ~ 5.8, temperature 45 ^{o}C, frequency 800 Hz, duty cycle 2:1, average current density 3 A/dm^2, stirring speed 200 ~ 500 r/min.

2.3. Heat treatment of plating sample

After the composite electrodeposition, the plated A3 samples were heat treated under argon atmosphere in a tube furnace. The specimen chamber was continuously flushed with sufficient argon during the heat treatment. The heating rate was 7 ^{o}C/min. The samples were maintained at 1100 ^{o}C for 3 h and then furnace-cooled to room temperature.

2.4. Microstructure and composition of the Ni-Al composite coating

The phase analysis of the Ni-Al composite coating was conducted by using X-ray diffraction (XRD) from the surface. Some of the specimens were mounted in the cold-setting epoxy resin to examine the cross-section using a scanning electron microscope (SEM) under backscattered electron image (BEI), and the distributions of elements in the various solid phases were analyzed by using an

energy dispersive X-ray spectroscope (EDS) attached in the SEM. The thickness of the coating varies between 100 and 150 μm, as determined by SEM.

2.5. Physical test of the Ni-Al composite coating

The adhesion strength of the coating on the A3 substrate was studied by the thermal shock test and File Test. The plated A3 samples were put into molten salt at 900 ^{o}C for 10 min and then water-quenched to room temperature. The thermal shock test was performed continuously for 10 times. The File Test employed a flat bastard file, which could be run across the coating surface to see if any of the coating could be removed.

2.6. Electrochemical test

The electrochemical behavior experiment of coating is tested in the simulated marine environment (2% 3% 4% 5% NaCl solution). The sodium chloride is obtained and guaranteed as analysis pure grade and the solution is prepared with twice-distilled water. The saturated calomel electrode (SCE) is employed as reference electrode to fabricate an integrated three-electrode mode. Pt as auxiliary electrode (1×2 cm^2) and the coated A3 steel as working electrode (10 mm×10 mm). The non-working surface is encapsulated with epoxy resin. The polarization curve is measured by potential scan from the relative corrosion potential -0.9V to -0.2V. AC excitation signal's amplitude, 5mV; frequency, 100mHz～100kHz; scanning speed, 1mV/s; number of sample, 30. Test results are indicated by Nyquist graph, and the AC impedance is fitted with EG&G attached Zsimpwin Version 310 fitting software with the instrument of Potentionstat/Galvanostat Model 263A potentiostat producted by EG&G company.

3. RESULTS AND DISCUSSION

3.1. The morphology and microstructure of the coating

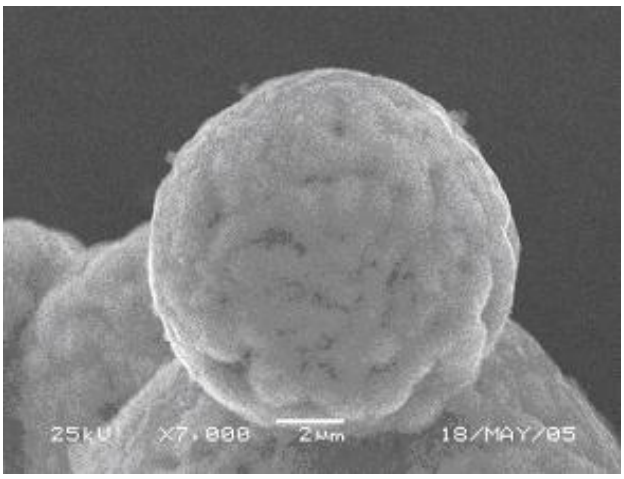

Figure 1. SEM micrograph of the surface morphology of a nickel-coated aluminum powder.

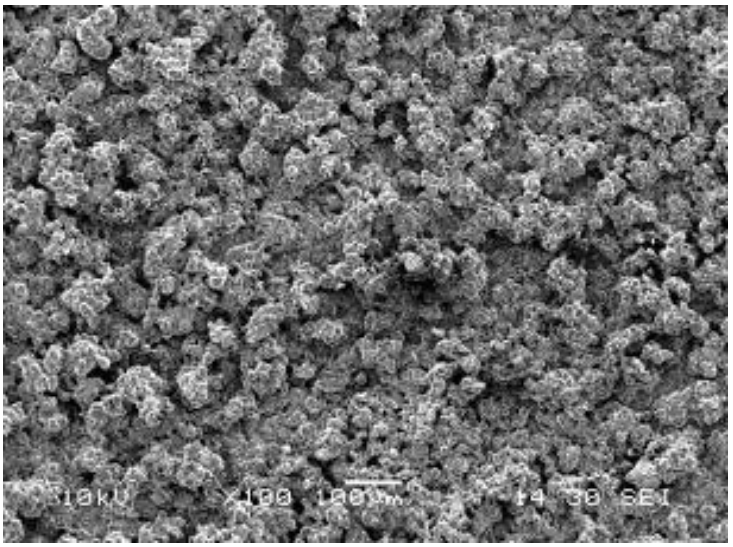

Figure 2. SEM micrograph of the surface morphology of the pulsed composite electrodeposition coating (before heat treatment).

The chemical plating results in the formation a layer of nickel on the aluminum powders, and the nickel layer is uniform and compact. Figure 1 shows the surface morphology of a nickel-coated aluminum powder. The surface morphology of the electrodeposited coating (before the heat treatment), as shown in Fig. 2, indicates that the nickel-coated particles distribute on the surface uniformly. During the composite electrodeposition, the cathodic polarization is largely eliminated by pulse current, so the hydrogen evolution and the amount of incompletely coated aluminum powders are reduced, which increases the content of the nickel-coated aluminum in the coating. The high current density also accelerates the rate of nickel deposition and improves the adsorbing ability of the substrate for the nickel-coated aluminum powders, but the content of nickel is increased [21].

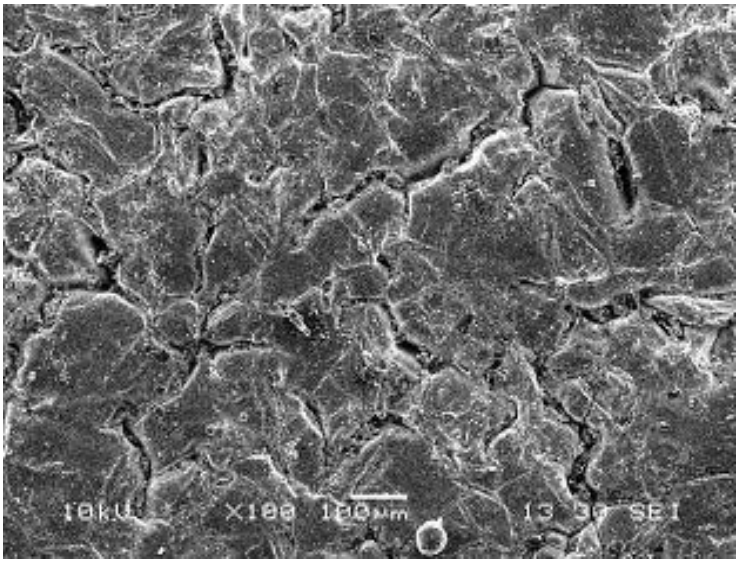

Figure 3. SEM micrograph of the surface morphology of the Ni-Al composite coating.

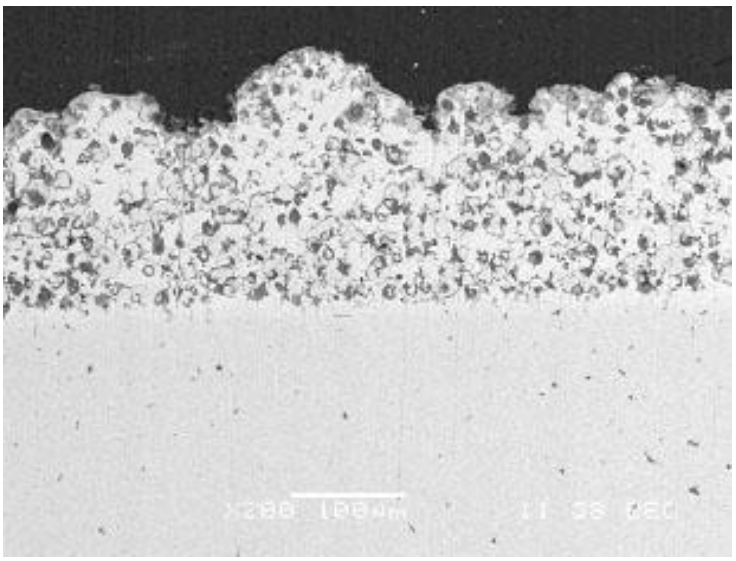

Figure 4. SEM micrograph of the cross-section morphology of the Ni-Al composite coating.

The surface morphology and the cross-section morphology of the Ni-Al composite coating (after the heat treatment) are shown in Figs. 3 and 4, respectively. The formation of the cracks on the coating surface might be attributed to the volume change of the electrodeposited coating, associated with the melting of aluminum and the diffusion of nickel and aluminum, during the heat treatment. However, these cracks do not penetrate through the coating to the substrate (Fig. 4). In fact, the Ni-Al composite coating is rather integrated implying that the coating is ductile enough to prevent cracking. The heat treatment under present condition does not develop a homogeneous Ni-Al intermetallic coating, but it results in the formation of a multi-phase coating composed of a continuous Ni-rich phase and discrete Al-rich particles enclosed in the Ni-rich phase. The distribution of the Al-rich particles is uniform.

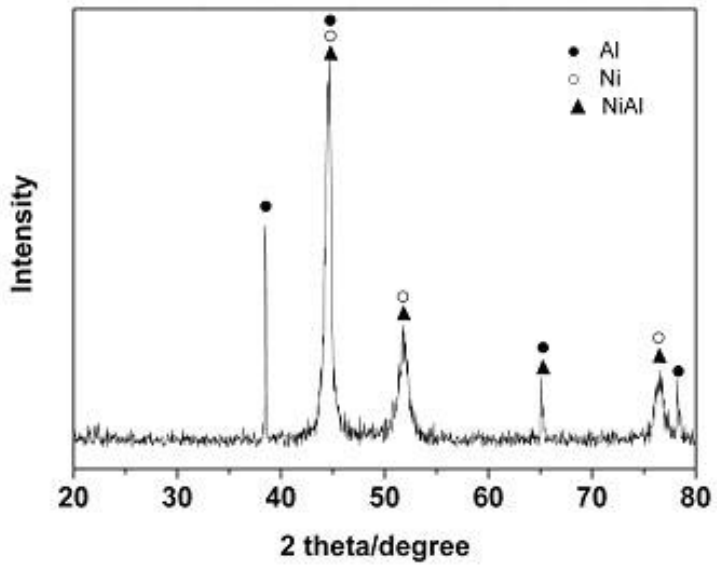

Figure 5. The surface XRD pattern of the Ni-Al composite coating.

The surface XRD pattern of the Ni-Al composite coating is shown in Fig. 5, which indicates that the coating consists mainly of phases Ni, Al, and NiAl intermetallics. It was reported that Ni-oxides grow much faster than alumina does at high-temperatures [22]. The absence of the fast-growing Ni-oxides peaks in the XRD pattern indicates that the Ni-Al composite coating forms alumina during the heat treatment. Again, the absence of the alumina peaks in the XRD pattern indicates that the content of alumina in the coating surface is low with respect to the detection limit of the XRD analysis. The thin protective alumina film, therefore, enables the Ni-Al composite coating to protect the A3 substrate against high-temperature corrosion.

After 10 runs of the thermal shock test, the Ni-Al composite coating does not detach from the A3 substrate. In addition, none of the coating is removed from the substrate after the File Test. According to the literature [23], the corrosion rate of Ni–Al coated alloy was lower than that of the uncoated alloy due to the formation of continuous, dense, adherent and protective oxide scale over the surface of the coatings. The formation of Ni-Al intermetallics between the coating and the A3 substrate might account for the excellent adhesion of the coating to the A3 substrate.

3.2. Polarization curve of coating

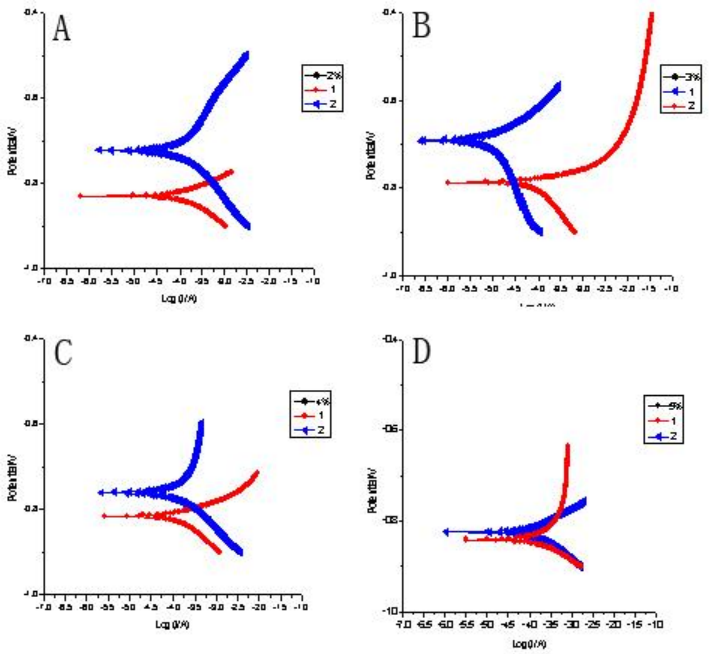

Figure 6. polarization curves of steel A3 and the coating in NaCl solution with different concentration ； 1：steel A3 2：steel A3 with coating A：2% NaCl solution B：3% NaCl solution C: 4% NaCl solution D: 5% NaCl solution

Polarization curves include anode polarization curve and cathode polarization curve. The crossing point of the cathode and anode polarization Tafel curves can be received by potential scan, and the corresponding potential and current are self-corrosion potential *E*corr and self-corrosion

current intensity *I*corr respectively. They can reflect the corrosivity of materials in corrosive medium and evaluate the protective effect of the coating [24].

The corrosion resistance of plain carbon steel and its composite Ni-coated Al coating are investigated in NaCl solution with different concentration.

Table 1. Corrosion parameters obtained from polarization curves shown in Fig. 6

	sample	E_{corr}（V）	J_{corr}（A/cm^2）
A	steel A3	-0.83	-5.90
	steel A3 with coatings	-0.72	-6.21
B	steel A3	-0.78	-6.63
	steel A3 with coatings	-0.69	-5.99
C	steel A3	-0.81	-5.70
	steel A3 with coatings	-0.76	-5.57
D	steel A3	-0.84	-5.99
	steel A3 with coatings	-0.82	-5.49

Self-corrosion potential of the coating is raised by about -0.1V compared to the matrix. The potential shifts towards the positive direction, while the self-corrosion current density is reduced more than two orders of magnitude, indicating that the coating can improve corrosion resistant of A3 steel obviously.

3.3. EIS of coating

The potentiostat can be programmed (under EIS function) to determine impedance spectra in a wide frequency range of 100mHz～100kHz. Effective area of the electrode specimen is 1 cm^2. The impedance spectra in different concentration are almost the same, hence take only one situation (3.5% NaCl solution) for example. The EIS of the coating and A3 steel are tested in 3.5% NaCl solution.

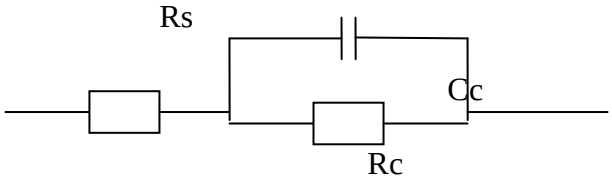

Figure 7. Electrical equivalent circuits used to fit the impedance spectra

Equivalent circuit fitting method is used to analyze the impedance in Fig.7 According to the literature [25]. Rs refers to solution resistant , while constant phase element (Cc) represents the ion transport resistant provided by coating, which depends on internal ion concentration and nature of the coating, porosity, structure of ion selective layer and ion transfer characteristic. Coating resistant (Rc) is a visual parameters that reflects the surface protective effect of the coating. Due to the coating impedance and corrosion current are in inverse relationship, higher impedance value can lead to better corrosion.

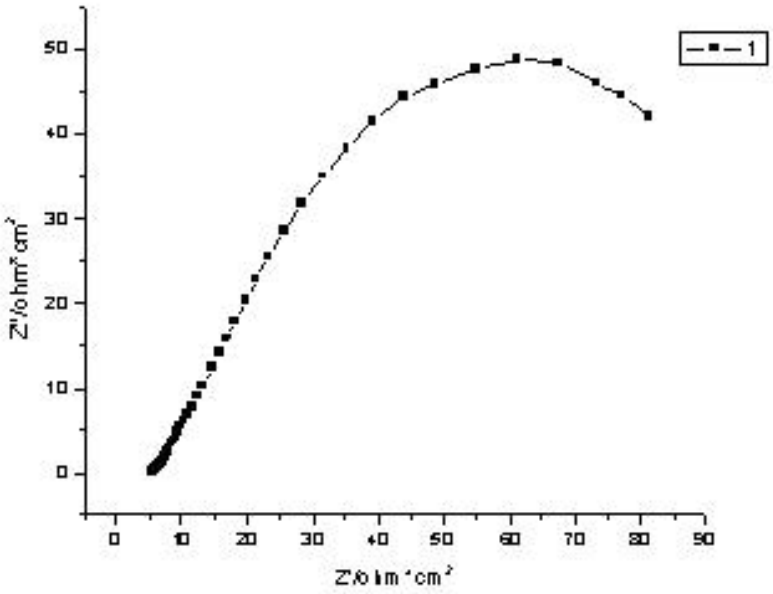

Figure 8. EIS of A3 steel without coatings

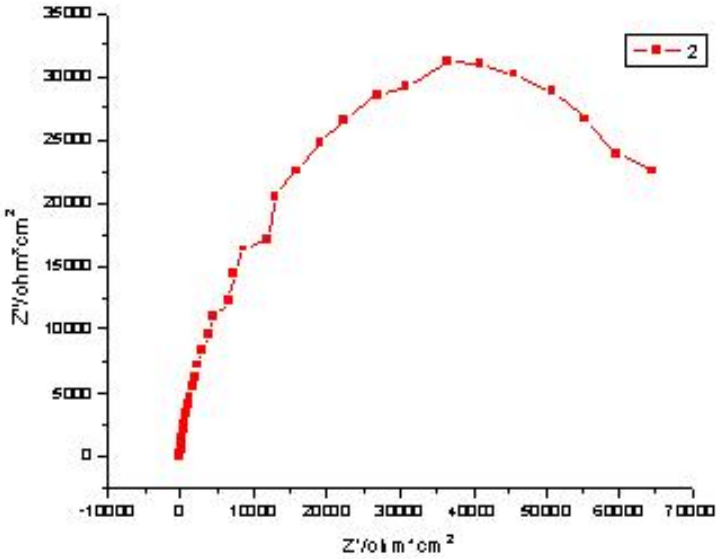

Figure 9. EIS of A3 steel with coatings

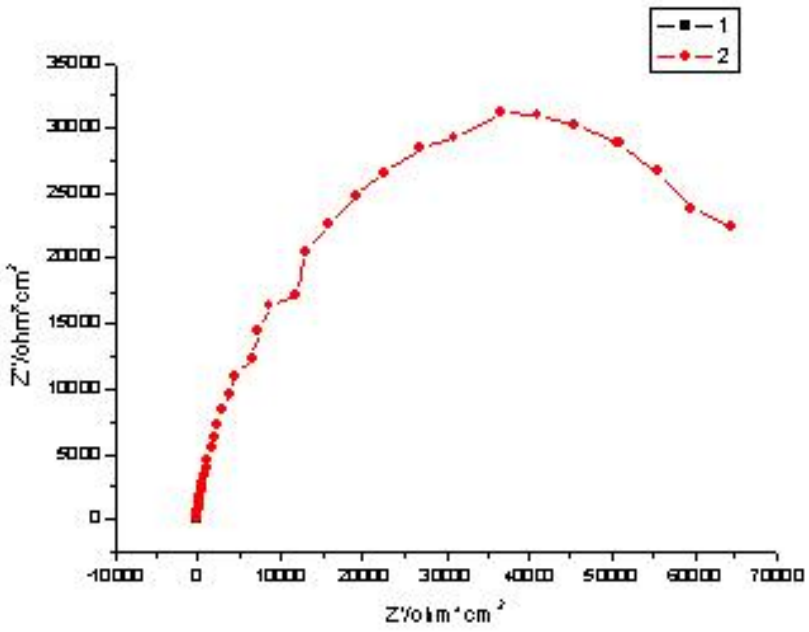

Figure 10. Stacking diagram of Fig. 8 and 9

Table 2. EIS fitting results for A3 steel with coatings and without coatings

sample	R（Ω.cm^2）
EIS of A3 steel without coatings	81.31
EIS of A3 steel with coatings	64590

The impedance value of the coating (64590 Ω • cm^2) is increased more than seven hundred times than the matrix (81.83 Ω • cm^2). Due to the impedance value is in inverse relationship with the corrosion current, the result is in accord with the polarization curve. As a result, the coating has excellent protection for A3 steel in marine environment.

3.4. Oxidation kinetics of the carbon steel A3

O_2 absorption properties were evaluated using a thermogravimetric instrument (TG; TG-DTA2500). The atmosphere was O_2 containing gases balanced by air, and kept for 1 h. The heating rate was 7 ^oC/min and the concentrations of O_2 were 5 %.

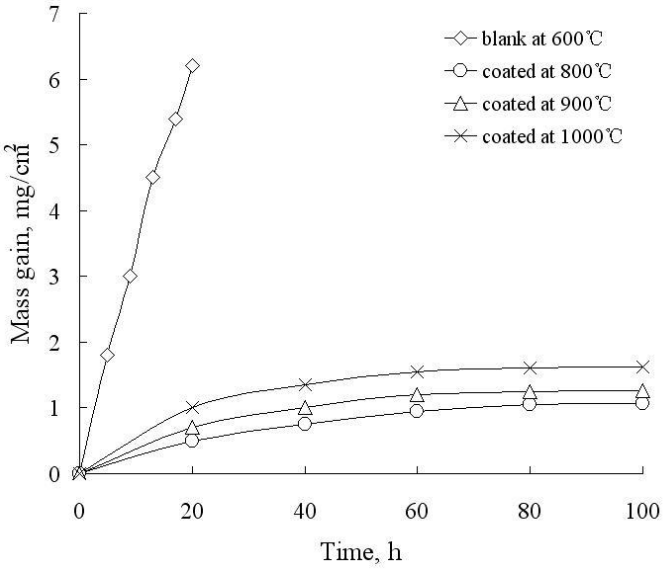

Figure 11. Oxidation kinetics of the carbon steel A3 with coatings and without coatings

Figure 11. shows the TG curves obtained at 600 ^{o}C in 5% O_2 gases for the substrate. The weight increase corresponds to the amount of O_2 absorption. It appeared that the slope of the tangent line at the beginning of absorption for the steel was much larger than that for the coating. Since the slopes correspond to absorption speed as reported in literature [26], the steel absorbed O_2 more than 8 times faster than the coating. The TG curves of the coated steel at 800, 900 and 1000 ^{o}C tend to gentle, which means the heat-resistant intermetallic compound has been formed to protect the steel.

4. CONCLUSIONS

The Ni-Al composite coating was prepared by using the pulsed composite electrodeposition and interdiffusion treatment on a low carbon steel. The coating is composed of a continuous Ni-rich phase and discrete Al-rich particles enclosed in the Ni-rich phase. The coating is crack-free and exhibits excellent adhesion to the steel substrate. The optimized processing parameters of the composite electrodeposition are as follows: duty cycle, 2; pulse frequency, 800 Hz; and current density, 3 A/dm^2. The polarization curve and EIS indicate that the coating can obviously improve corrosion resistant of A3 steel in marine environment. The thickness of the coating with 100~150 μm can provide good protection to A3 steel.

References

1. J. Mackowiak, N.R. Short, *Int. Mater. Rev*. 24 (1979) 1-19.
2. Amit Kumar Gupta, D. Ravi Kumar, *J. Mater. Process. Technol*. 172 (2006) 225-237.
3. C.E. Jordan, R. Zuhr, A.R. Marder, *Metall. Mater. Trans*. A. 28 (1997) 2695-2703.
4. P.R. Seré, M. Zapponi, C.I. Elsner, A.R. Di Sarli, *Corros. Sci*. 40 (1998) 1711-1723.
5. S.M.A. Shibli, R. Manu, V.S. Dilimon, *Appl. Surf. Sci*. 245 (2005) 179-185.

6. F. García, A. Salinas, E. Nava, *Mater. Lett*. 60 (2006) 775-778.
7. R.W. Richards, R.D. Jones, P.D. Clements, H. Clarke, *Int. Mater. Rev*. 39 (1994) 191-212.
8. D.Q. Wang, *Appl. Surf. Sci*. 254 (2008) 3026-3032.
9. C. Müller, M. Sarret, T. Andreu, *Electrochim. Acta* 48 (2003) 2397-2404.
10. M.E. Bahrololoom, D.R. Gabe, G.D. Wilcox, *J. Electrochem. Soc*. 150 (2003) C144-C151.
11. Z. Zhang, W.H. Leng, H.B. Shao, J.Q. Zhang, J.M. Wang, C.N. Cao, *J. Electroanal. Chem*. 516 (2001) 127-130.
12. J.B. Bajat, V.B. Mišković-Stanković, M.D. Maksimović, D.M. Dražić, S. Zec, *Electrochim. Acta* 47 (2002) 4101-4112.
13. M.M. Younan, J. Appl. Electrochem. 30 (2000) 55-60.
14. H. Ashassi-Sorkhabi, A. Hagrah, N. Parvini-Ahmadi, J. Manzoori, *Surf. Coat. Technol*. 140 (2001) 278-283.
15. R. Ramanauskas, L. Gudavičiūtė, A. Kaliničenko, R. Juškėnas, *J. Solid State Electrochem*. 12 (2005) 900-908.
16. D.F Susan, A.R Marder, *Acta Mater*. 49 (2001) 1153-1163.
17. D.F Susan, A.R Marder, *Oxid. Met*. 57 (2002) 159-180.
18. Y.B. Zhou, X. Peng, F.H. Wang, *Oxid. Met*. 64 (2005) 169-183.
19. H.F. Liu, W.X. Chen, *Surf. Coat. Technol*. 191 (2005) 341-350.
20. H.F. Liu, W.X. Chen, *Surf. Coat. Technol*. 202 (2008) 4019-4027.
21. S. Esmaili, M.E. Bahrololoom, *Surf. Eng. Appl. Electrochem*. 48 (2012) 35-41.
22. Y. Wu, F. Gesmundo, Y. Niu, *Oxid. Met*. 65 (2006) 53-74.
23. A. Rahman, R. Jayaganthan, S. Prakash, V. Chawla, R. Chandra, *J. Alloys Compd*. 472(2009)478-483.
24. Cissé, M Abouchane, T Anik, K Himm, *Int.J.corros*. 10(2010)1155-1164.
25. Chengfei Zhu, Rui Xie, Jinhua Xue, Linlin Song, *Electrochim. Acta.* 16(2011)5828–5835.
26. Q. Feng, T. J. Li, H. Teng, X. L. Zhang, Y. Zhang, *Surf. Coat. Technol*. 17(2008)4137-4144.